Real-time Continuous Blood Pressure Estimation with Contact-free Bedseismogram

Abstract—In this study, we introduce BedDot, the first contact-free and bed-mounted continuous blood pressure monitoring sensor. Equipped with a seismic sensor, BedDot eliminates the need for external wearable devices and physical contact, while avoiding privacy or radiation concerns associated with other technologies such as cameras or radars. Using advanced pre-processing techniques and innovative AI algorithms, we extract time-series features from the collected bedseismogram signals and accurately estimate blood pressure with remarkable stability and robustness. Our user-friendly prototype has been tested with over 75 participants, demonstrating exceptional performance that meets all three major industry standards, which are the Association for the Advancement of Medical Instrumentation (AAMI) and Food and Drug Administration (FDA), and outperforms current state-of-the-art deep learning models for time series analysis. As a non-invasive solution for monitoring blood pressure during sleep and assessing cardiovascular health, BedDot holds immense potential for revolutionizing the field.

Index Terms—blood pressure, circadian rhythm, contact-free sleep monitoring, deep neural network, seismic sensing, sleep

Fig. 1. Installation of BedDot under the bed frame.

I. INTRODUCTION

Several studies [1], [2] highlight the strong links between systolic blood pressure (SBP), diastolic blood pressure (DBP), sleep, aging, and the prevalence of cardiovascular and vascular diseases. As of 2016, there were approximately 47.8 million individuals 65 years and older in the United States, with 26% living alone at home and 18% residing in senior healthcare facilities according to the U.S. Census Bureau. The growing aging population will only exacerbate the impact of uncontrolled hypertension on the health and well-being of society, as well as contribute to skyrocketing healthcare costs. Real-time blood pressure monitoring during sleep is crucial, even life-saving, for those suffering from hypertension-related diseases such as heart attacks, strokes, heart failure, and kidney disease. Polysomnography, a standard sleep clinic technology, is able to continuously detect physiological abnormalities overnight, while it is both costly and inaccessible to families. Most commercial alternatives, such as wearable sensors and wrist devices, require bodily contact and can be intrusive. Furthermore, the use of cameras or radars to monitor in-bed body motion raises privacy concerns [3] or radiation concerns. A contact-free and non-intrusive solution to monitor blood pressure would have far-reaching benefits for individuals and healthcare providers alike. By allowing individuals to self-manage their health and share the results with their healthcare providers, diseases can be managed more effectively. This would be a revolutionary development, as millions of Americans suffer from complex diseases that remain uncontrolled, leading to preventable complications and deaths each year.
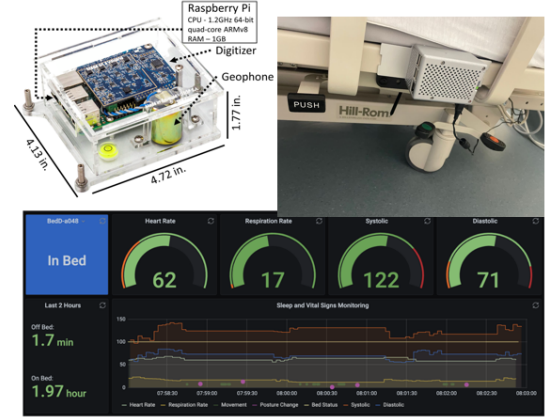
In this study, we use BedDot, a contact-free sleep monitoring system that can continuously monitor sleep and vital signs without the need for instrumentation on the body. BedDot uses a seismic sensor mounted on the bed to collect real-time bedseismogram (BSG) signals, which measure microvibrations on the bed frame that are induced by heart movement, respiration, and blood pressure changes. This technology is not new, as seismic signals have been widely used in geophysical and civil engineering fields for many years [4], and more recently, in analyzing human health conditions [5]. For example, the seismocardiogram (SCG) signals created by chest vibration have been used to extract heartbeat and implement user authentication on mobile phones [6]. Based on a bed-mounted geophone, researchers monitored heart rate during sleep [7]. More recently, a vertical geophone with a 2.5 kHz sampling frequency was used to implement both heart rate and respiration rate monitoring [8]. However, there has been limited research on real-time blood pressure monitoring using vibration signals. Although it is not straightforward that the vibration signals are directly connected to the blood pressure predictions, [9] indicates that the blood pressure and the blood volume flow predictions can be done by using the ballistocardiograph (BCG) signals, which share the same idea as our BSG signals. Therefore, we introduced two machine learning models to reveal this non-obvious connection between the BSG signals and the blood pressure.

The BedDot system, as illustrated at the top of Figure 1, is easily set up by attaching it to a bed frame. The system consists of a Raspberry Pi 3 and an ADC that connects to the seismometer and saves raw data to a local database.

The hardware of BedDot is shown in Figure 1. In addition to monitoring on/off bed detection, sleep posture, and heart and respiration rates [8], BedDot is capable of monitoring blood pressure during sleep, making it a unique and effective solution. The monitoring dashboard is also shown at the bottom of Figure 1. To the best of our knowledge, this is the first work that proposes a contact-free system for blood pressure monitoring during sleep using BSG signals.

The BedDot system is powered by advanced AI algorithms that can accurately estimate real-time blood pressure. The system proposes two novel and reliable methods for blood pressure estimation, both of which use time-series features extracted from BSG signals. The first method is a convolution-recurrent hybrid neural network model, which leverages convolutional neural network (CNN) components to learn representations from the input high-dimensional time-series features, and bidirectional long short-term memory (LSTM) components to model the temporal dependencies. The second method is called Vital Temporal Convolutional Networks (VTCN) and is based on a modified causal convolutional architecture. Unlike existing vital sign estimation methods [10], which require a single data analysis window of 30-120 seconds, the BedDot system continuously monitors changes in SBP/DBP using a seismometer with a 100 Hz sampling frequency and collects the BSG signal caused by bed vibrations, allowing for data segments of 10 seconds. This makes the system more suitable for real-time blood pressure monitoring during sleep and even clinical studies.

The major contributions of this paper can be summarized as follows. **(1)** The proposed algorithms are the first successful attempt to estimate continuous blood pressure during sleep without physical contact. BedDot, a bed-mounted seismic sensor, is used to measure micro-vibrations on the bed frame that are induced by heart movement, respiration, and blood pressure changes. With a high sampling frequency, the system can generate real-time time-series features and estimate blood pressure in real time. This innovative approach offers a contact-free method of monitoring blood pressure, which could be beneficial for those with cardiovascular diseases, cognitive disorders, or other medical conditions that require continuous monitoring. **(2)** This paper proposes blood pressure estimation methods based on advanced AI algorithms that meet the criteria for evaluating commercial blood pressure measuring devices. The performance of these algorithms is then compared to state-of-the-art deep learning models for time-series analysis. Numerical results show that the proposed AI models are superior to the existing models. This demonstrates the potential of AI algorithms to accurately measure blood pressure with high levels of accuracy.

II. Data collection and data quality control

A. Data collection

In this paper, BedDots were utilized to detect mini-vibrations on the surface they were attached to. The sampling rate is 100 Hz. The data were collected in a controlled setting at the University of Georgia Clinical and Translational Research Unit (CTRU) using a standard hospital bed and a family bed. Two BedDots were installed on each bed. The main difference between the two types of beds is the bed frame and mattress, which could affect the propagation of vibration waves. Each data sample consisted of a 10-second recorded BSG signal. The true values of the blood pressure were collected by using the FDA-approved wearable device at the same time during the experiment and were used as the ground truth blood pressure measurements, which represent the real blood pressure of the participants. We then evaluated our blood pressure predictions by comparing them with the ground truth.

B. Data quality control

The BSG signal collected by BedDot is composed of various vibration sources, such as background white noise, home environment noises from appliances (e.g. air conditioner, washer, dryer), body movements during sleep, and vibrations caused by vital activities like heartbeat, respiration, and blood pressure changes. To accurately estimate blood pressure, we filter out vibrations that do not reflect vital activities. We use an automatic signal processing algorithm to eliminate signals with "bad quality". For each 10-second segment, we measure its spectral distance, energy standard deviation, and standard deviation. If one of the following three thresholds is triggered, the signal segment is labeled as "bad quality" and filtered out: spectral distance is less than 7, energy standard deviation is less than 18, and the standard deviation is greater than 5. Small spectral distance or energy standard deviation indicates behavior similar to white noise and usually lacks meaningful information on vital activities. On the other hand, a signal segment with a large standard deviation is usually dominated by a body movement like changing sleep posture, which is much stronger than common vital activities. These thresholds are based on our experience with BSG signal processing [10], [11]. To further filter out nuisance information, we check the frequency domain. Figure 2 shows a 5-minute recorded vibration data. The available frequency range is 0-50 Hz, based on the seismometer's 100 Hz sampling rate and the Nyquist sampling theorem. The red dashed frame represents the background noise with varying dominant frequencies, while the blue dashed frame denotes machine vibrations from a dryer with an 11 Hz dominant frequency and harmonics at 22 Hz and 33 Hz. To remove these machine noises, we first apply a spectrum scanning method, then use notch filters to suppress the noise components with iso-dominant frequencies.

In addition, we follow the recommendation in [12] to remove data with irregular pulse pressure (the difference between SBP and DBP). A high pulse pressure, e.g. greater than 60 mmHg (millimeters of mercury), is usually considered an indicator of an immediate heart problem [13]. On the other hand, a low pulse pressure, say beneath 20 mmHg, may be a sign of poor heart function [14]. In our case, we only consider taking quality control of the higher bound. So, the upper bound of 60 mmHg is the conservative limit to filter out outliers that may inaccurately represent blood pressure anomalies. We
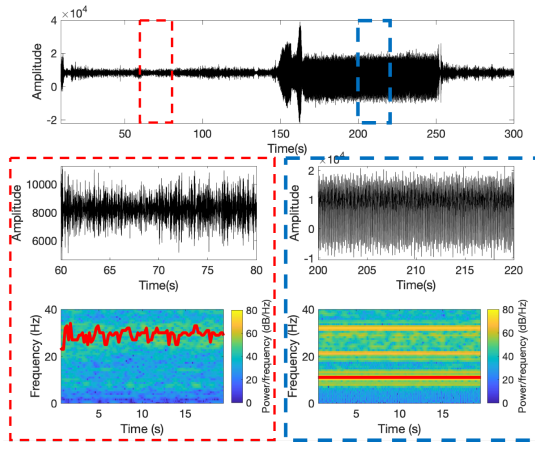
Fig. 2. Background noise and machine vibration in BSG signals.

summarize the flow chart of the proposed data collection, preprocessing, and estimation procedure in Figure 3.
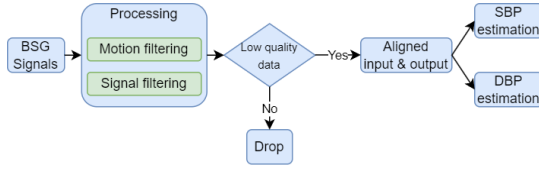

Fig. 3. SBP/DBP estimation workflow.

III. BLOOD PRESSURE ESTIMATION METHODS

In this section, we introduce two novel deep-learning methods for estimating blood pressures (SBP and DBP) from the collected 100 Hz BSG signals. Section III-A introduces a novel hybrid model that combines a CNN and an LSTM network. Section III-B presents a VTCN model. In Section III-C, we provide implementation details and discuss hyperparameter selection for both methods.
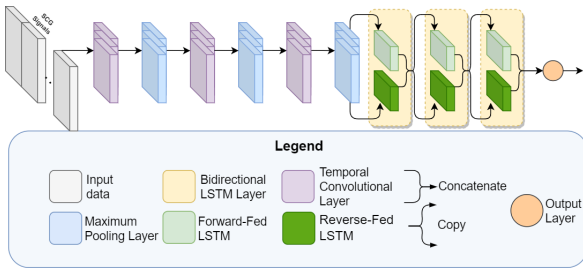

Fig. 4. Architecture of the proposed CNN-LSTM hybrid model.

A. CNN-LSTM hybrid model

In this subsection, we present a CNN-LSTM hybrid model, as illustrated in Figure 4. The CNN component is a feed-forward neural network that leverages local receptive fields, shared weights, and pooling to significantly reduce the number of parameters in fully connected neural networks, enabling dimensionality reduction and feature extraction. 1D-CNNs have been widely used in electrocardiogram anomaly detection [12]

and are well-suited for real-time, low-cost applications due to their low computational requirements.Our model has 3 temporal convolutional layers of 128 feature maps, each followed by a max pooling layer, with a receptive field size of 3 and rectified Linear Unit (ReLU) activation.

To be specific, the convolution process can be expressed as $x_k^l = b_k^l + \sum_{i=1}^{N_{l-1}} conv1D(w_{ik}^{l-1}, s_i^{l-1})$, where x_k^l represents the input, b_k^l is a scalar bias of the k-th neuron at layer l, and s_i^{l-1} is the output of the i-th neuron at layer $l-1$. Moreover, w_{ik}^{l-1} is the kernel from the i-th neuron at layer $l-1$ to the k-th neuron at layer l. Therefore, y_k^l, the output of the neuron, can be expressed by the activation function of x_k^l, i.e. $y_k^l = f(x_k^l)$, where f is the ReLU activation function.

Each pooling layer utilizes a 1-D max-pooling with a window size of 8 and a stride length of 2. Max-pooling reduces the dimensions of the input representation by taking the maximum value within the defined pool size window. This helps to downsample the output of the convolutional layer and prevent overfitting. The max pooling operation can be described as $s_k^l = y_k^l \downarrow ss$, where s_k^l is the output of the maximum pooling layer and $\downarrow ss$ represents the downsampling operation conducted by a maximum pooling layer.

Our model also incorporates three bidirectional LSTM layers after the convolutional section. Bidirectional LSTMs access the data in both forward and backward directions by combining a forward-fed layer and a reverse-fed layer. This allows the LSTMs to learn from values both in the past and future within the sequence. Both directions are performed similarly to a standard LSTM, and their outputs are then concatenated to provide the overall result. In our experiments, we use the Adam optimization algorithm [15] with a learning rate of 0.001. The final layer is a fully connected dense layer, which provides the final output of the network. During training, 90% of the training set was used for model training and 10% was set aside as the validation set.

B. VTCN model

The temporal Convolution Model (TCN) [16] is a member of the Convolutional Neural Network (CNN) family. Unlike traditional CNNs, TCNs employ a causal convolution, meaning that the convolution process at time t only depends on observations prior to time t, thus avoiding the issue of "information leakage." Furthermore, TCNs use dilated convolutions, which enables the model to capture information over a longer history with an exponentially larger receptive field compared to non-dilated causal convolutions. In essence, TCNs can be considered as the combination of 1D fully-convolutional networks and causal convolutions [16]. To be more specific, for a 1D sequence input $\boldsymbol{X} \in \mathbb{R}^n$ and a filter f: $\{0, 1, ..., k-1\} \rightarrow \mathbb{R}$, the dilated convolution operation F on elements s of the sequence is defined as $F(s) = (\boldsymbol{X} *_d f)(s) = \sum_{i=0}^{k-1} f(i) \cdot \boldsymbol{X}_{s-d\cdot i}$, where d is the dilation factor, k is the filter size, and $s - d \cdot i$ represents the direction of the past.

Our VTCN model consists of a series of blocks, with each block containing a sequence of convolutional layers. We use j to denote the number of blocks and l for the number of

layers within a block. The dilation rate d increases by a factor of 2^l for consecutive layers. The activations in the l-th layer and j-th block are represented as $S^{j,l} \in \mathbb{R}^{F \times T}$, where F is the number of filters and T is the number of corresponding time steps. The input for each block $S^{j,l}$ is the output from the previous block $S^{(j-1,l)}$, with the exception of the first block, which receives the input data. We propose a modified TCN model, referred to as the Vital TCN or VTCN, which includes an additional batch normalization layer and ReLU activation function in each block of the classical TCN model. Additionally, we have added a linear layer at the end of the layers to make the model suitable for regression.

C. Implementation and hyperparameter selection

In our experiments, BSG signal observations are treated as a time series, indexed by collection time. We allocate 70% of these observations to the training set and 30% to the test set. A validation set, representing 10% of the training sample, is derived after sorting daily samples by timestamps. So, there is neither overlapping nor information leakage. For the CNN-LSTM hybrid model, both the train set and the test set are normalized using the training set's mean and standard deviation, ensuring no data leakage. The VTCN model doesn't require normalization. Our CNN-LSTM model uses Keras, a Python deep learning API, while the VTCN model employs PyTorch by Meta AI. Both models undergo training and validation over 150 epochs using mean absolute error (MAE) as the loss function. Weights are optimized for each epoch to minimize the validation set's MAE. Post-training, weights yielding the lowest MAE are used for testing.

IV. EXPERIMENTS AND EVALUATIONS

We evaluate the performance of the BedDot system in real-time, contact-free blood pressure estimation. The quality control measures described in Section II were followed to produce a preprocessed dataset of 33,982 observations collected from more than 75 participants over 43 days. True systolic blood pressure (SBP) and diastolic blood pressure (DBP) measurements were obtained using a United States Food and Drug Administration (FDA) approved clinical blood pressure monitor, following established clinical techniques. The histograms of SBP and DBP are shown in Figure 5, with sample means of 120 mmHg and 70 mmHg, respectively. The dataset was divided into two parts: first 70% of the daily data was used for training, and the remaining 30% was used for testing. So there is no overlapping and data leakage issues between training and testing sets. A 10-fold cross-validation was used in modeling tuning and the validation sets were split from the training set. Both the CNN-LSTM hybrid model and the VTCN model were trained on the training set, following the model training and hyperparameter selection methods outlined in Section III-C. The trained models were then used to predict SBP and DBP on the testing set. The prediction error was evaluated using mean absolute error (MAE), standard deviation (SD), and mean absolute percentage difference (MAPD). In addition, we compare the performance of the two proposed AI models with several state-of-the-art deep learning methods for time

series data. The accuracy of the blood pressure estimation was evaluated using two widely accepted criteria: the Association for the Advancement of Medical Instrumentation (AAMI) standard [17] and ISO 81060-2-2018 from the U.S. FDA.
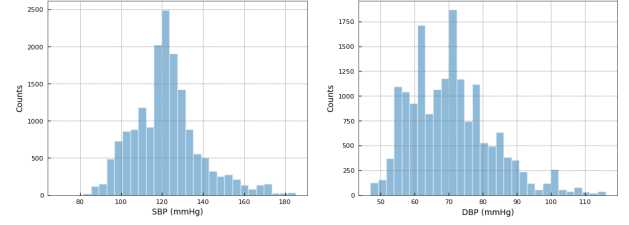

Fig. 5. Histograms for SBP (top panel) and DBP (bottom panel)

A. Analysis of experiment results

In Table I, we report MAE, SD, 95% confidence interval of MAE, and the correlation coefficient between the predicted values and the truth. The results in Table I show both the CNN-LSTM hybrid model and the VTCN model achieve small MAE and SD in terms of SBP and DBP estimations. In addition, the predictions made by both models have high correlation coefficients with the truth. The CNN-LSTM hybrid model slightly outperforms the VTCN model as it has lower MAE and SD for both SBP and DBP. In general, the estimation errors for DBP are lower than SBP as DBP has a smaller scaling than SBP. Figure 6 presents error histograms that visualize the empirical distributions of prediction errors. The error histograms show the predictions errors of both models are symmetric to and tightly concentrate around 0. Besides, the tails of error empirical distributions decay to zero very fast which is another evidence of good prediction performance. Again, we find the peak in the error histogram of the CNN-LSTM hybrid model is higher than the VTCN model. This is in line with our observation in Table I that the CNN-LSTM hybrid model slightly outperforms the VTCN.

In Table I, we present the results of MAE, SD, 95% confidence interval of MAE, MAPD, and the correlation coefficient ρ between the predicted and true values. Our results indicate that both the CNN-LSTM hybrid model and the VTCN model exhibit low MAE and SD for both systolic and diastolic blood pressure estimations. Additionally, the predictions made by both models have high correlations with the truth. The CNN-LSTM hybrid model slightly outperforms the VTCN model as it has lower MAE and SD for both systolic and diastolic blood pressure. On average, the estimation errors for diastolic blood pressure are lower than those for systolic blood pressure as diastolic blood pressure has a smaller scale. Figure 6 displays error histograms that visualize the distribution of prediction errors. The histograms indicate that the prediction errors for both models are symmetric and tightly concentrated around 0. Moreover, the tails of the error distributions decay rapidly to zero, indicating good prediction performance. In line with our findings in Table I, the peak of the error histogram for the CNN-LSTM hybrid model is higher than that for the VTCN

model, suggesting that the CNN-LSTM hybrid model slightly outperforms the VTCN model.

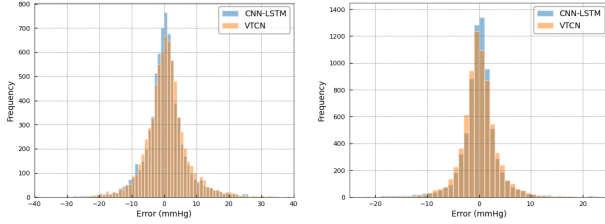|		MAE	SD	95% CI	MAPD	ρ
VTCN	SBP	4.80	5.39	(4.69, 4.91)	3.97	0.91
	DBP	2.57	3.06	(2.51, 2.63)	3.70	0.95
CNN-LSTM	SBP	4.66	5.76	(4.54, 4.78)	3.87	0.90
	DBP	2.67	3.89	(2.59, 2.75)	3.83	0.92

Fig. 6. Error histograms for SBP (top panel) and DBP (bottom panel).

In the Bland-Altman plot (also known as the Tukey mean-difference plot), we evaluate the agreement between two arrays of data, such as the predicted values and the ground truth. Figure 7 presents the Bland-Altman plots for SBP and DBP predictions. The dense cluster of points near the "difference = 0" line indicates a strong agreement between the predicted values and the truth. The blue and orange dotted lines represent the limits of agreement for the CNN-LSTM hybrid model and VTCN model, respectively. For the CNN-LSTM hybrid model, 94.76% and 95.19% of points fall within the limits of agreement for SBP and DBP, respectively. For the VTCN model, 94.46% and 95.18% of points fall within the limits of agreement for SBP and DBP, respectively. These results suggest a high level of agreement between the true blood pressures and the predictions made by the models.
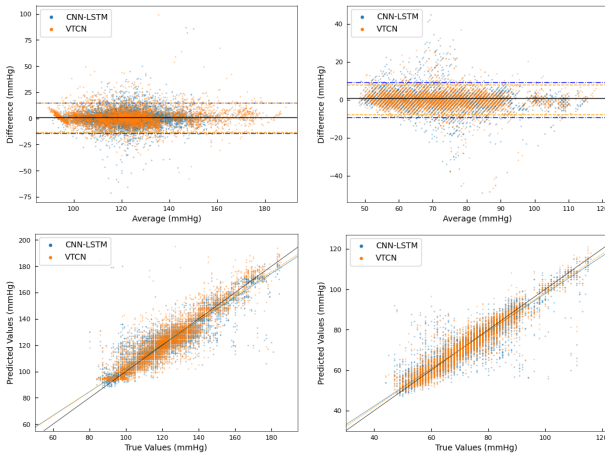

Fig. 7. Bland Altman plots for SBP (top left) and DBP (top right).Regression plots for SBP (bottom left) and DBP (bottom right).

In Figure 7, scatter plots are used to demonstrate the agreement level between the sorted true blood pressures and their corresponding predictions made by the proposed models. The solid black line indicates the theoretical "perfect" correlation, while the orange and blue dashed lines depict the actual correlation coefficients (as listed in Table I) of the CNN-LSTM hybrid model and the VTCN model, respectively. The scatter plots reveal a strong positive correlation between the true blood pressure and the predictions generated by the models. The calculated correlation lines are close to the "perfect" correlation line in the area where the majority of data points are concentrated. Based on the analysis, there is strong evidence to support the accuracy of the CNN-LSTM hybrid model and VTCN model in estimating SBP and DBP using the BSG signals collected by the BedDot system. The strong correlation between the predictions and the truth demonstrates the effectiveness of our system.

B. Evaluation metrics

We describe two well-established criteria used to evaluate and grade blood pressure monitoring devices based on their estimation accuracy. The American Association for the Advancement of Medical Instrumentation (AAMI) published a monograph in 1987, which became a national standard for the evaluation of sphygmomanometers. This monograph included a standard for evaluating the accuracy of blood pressure monitoring devices, which are generated through a consensus process by committees of experts in research, development, and design from user, industry, and government communities [17]. According to the AAMI standard, a blood pressure monitoring device is considered to "pass" if its blood pressure estimation satisfies MAE $\leq$ 5 mmHg and SD $\leq$ 8 mmHg [18]. The U.S. Food and Drug Administration (FDA) evaluation criteria ISO 81060-2:2018(E) suggest that the mean of the errors of the paired determinations of the sphygmomanometer-under-test for all subjects should be within or equal to ± 5.0 mmHg, with an experimental standard deviation no greater than 8.0 mmHg [19]. We also report the mean absolute percentage difference (MAPD) as a reference in accordance with the IEEE standard for device accuracy. This provides a measure of the stability of our predictions.

C. Comparison with existing methods

Our CNN-LSTM and VTCN models were compared with leading deep learning methods for time series analysis, namely Multilevel Wavelet Decomposition Network (mWDN) [20], 1D-ResCNN (ResCNN) [21], Recurrent Neural Network and Fully Convolutional Network (RNN-FCN) [22], Explainable Convolutional Neural Network (XCM) [23], and Time-series Transformer (TST) [24]. All models underwent identical training, validation, and testing protocols. Table II shows the evaluation results of our models and the five competing methods using the AAMI standard and the FDA standard. The results demonstrate that none of the five competing methods met the AAMI criteria for SBP estimation, with only RNN-FCN achieving the AAMI standard for DBP estimation. Conversely, both our CNN-LSTM and VTCN models surpassed the AAMI benchmark for SBP and DBP estimations and displayed the smallest mean absolute errors. In summary, CNN-LSTM and

VTCN excel in meeting both AAMI and FDA standards, outclassing all other methods in accuracy and consistency.

TABLE II
COMPARISON OF SBP AND DBP ESTIMATIONS BASED ON THE AAMI
STANDARD AND FDA STANDARD

		Absolute difference (mmHg)				
		MAE	SD	MAPD	AAMI	FDA
TST	SBP	12.50	11.39	10.45	fail	fail
	DBP	9.82	7.72	14.0	fail	fail
mWDN	SBP	12.15	10.55	10.04	fail	fail
	DBP	8.88	7.01	12.84	fail	fail
ResCNN	SBP	9.88	8.74	8.19	fail	fail
	DBP	6.30	5.95	8.85	fail	fail
XCM	SBP	10.15	8.83	8.40	fail	fail
	DBP	7.09	6.19	10.13	fail	fail
RNN-FCN	SBP	6.46	6.21	5.33	fail	fail
	DBP	4.19	3.99	6.03	pass	pass
VTCN	SBP	4.80	5.39	3.97	pass	pass
	DBP	**2.57**	**3.06**	**3.70**	pass	pass
CNN-LSTM	SBP	**4.66**	**5.76**	**3.87**	pass	pass
	DBP	2.67	3.89	3.83	pass	pass

V. CONCLUSION

In this study, we introduced a pioneering approach to continuous, contactless blood pressure monitoring using a bed-mounted seismic sensor (BedDot) and two AI models. Our experiments, conducted in both controlled hospital settings and real-world conditions, demonstrated the efficacy of our algorithm in real-time systolic and diastolic blood pressure estimation. Our models surpassed five leading deep learning-based time series models in accuracy and consistency. However, the VTCN and CNN-LSTM methods still require further evaluation for Out-Of-Distribution (OOD) generalization. Further investigations are underway to validate these findings.

REFERENCES

[1] S.-M. Hakala, R. Tilvis, and T. Strandberg, "Blood pressure and mortality in an older population: a 5-year follow-up of the helsinki ageing study," *European heart journal*, vol. 18, no. 6, pp. 1019–1023, 1997.

[2] M. Gurven, A. D. Blackwell, D. E. Rodríguez, J. Stieglitz, and H. Kaplan, "Does blood pressure inevitably rise with age? longitudinal evidence among forager-horticulturalists," *Hypertension*, vol. 60, no. 1, pp. 25–33, 2012.

[3] F. Zhao, Z. Cao, Y. Xiao, J. Mao, and J. Yuan, "Real-time detection of fall from bed using a single depth camera," *IEEE Transactions on Automation Science and Engineering*, vol. 16, no. 3, pp. 1018–1032, 2018.

[4] F. Li, Y. Qin, and W. Song, "Waveform inversion-assisted distributed reverse time migration for microseismic location," *IEEE Journal of Selected Topics in Applied Earth Observations and Remote Sensing*, vol. 12, no. 4, pp. 1327–1332, 2019.

[5] W. Chen, M. Guan, Y. Huang, L. Wang, R. Ruby, W. Hu, and K. Wu, "A low latency on-body typing system through single vibration sensor," *IEEE Transactions on Mobile Computing*, pp. 1–12, 2019, Online.

[6] L. Wang, K. Huang, K. Sun, W. Wang, C. Tian, L. Xie, and Q. Gu, "Unlock with your heart: Heartbeat-based authentication on commercial mobile phones," *Proceedings of the ACM on Interactive, Mobile, Wearable and Ubiquitous Technologies*, vol. 2, no. 3, p. 140, 2018.

[7] Z. Jia, M. Alaziz, X. Chi, R. E. Howard, Y. Zhang, P. Zhang, W. Trappe, A. Sivasubramaniam, and N. An, "HB-phone: a bed-mounted geophone-based heartbeat monitoring system," in *Information Processing in Sensor Networks (IPSN), 2016 15th ACM/IEEE International Conference on*. IEEE, 2016, pp. 1–12.

[8] Z. Jia, A. Bonde, S. Li, C. Xu, J. Wang, Y. Zhang, R. E. Howard, and P. Zhang, "Monitoring a person's heart rate and respiratory rate on a shared bed using geophones," 2017.

[9] C.-S. Kim, S. L. Ober, M. S. McMurtry, B. A. Finegan, O. T. Inan, R. Mukkamala, and J.-O. Hahn, "Ballistocardiogram: Mechanism and potential for unobtrusive cardiovascular health monitoring," *Scientific reports*, vol. 6, no. 1, p. 31297, 2016.

[10] F. Li, M. Valero, J. Clemente, Z. Tse, and W. Song, "Smart sleep monitoring system via passively sensing human vibration signals," *IEEE sensors journal*, vol. 21, no. 13, 2021. [Online]. Available: http://sensorweb.engr.uga.edu/wp-content/uploads/2021/07/li2021smart.pdf

[11] M. Valero, J. Clemente, F. Li, and W. Song, "Health and sleep nursing assistant for real-time, contactless, and non-invasive monitoring," *Pervasive and Mobile Computing*, vol. Volume 75, 2021. [Online]. Available: http://sensorweb.engr.uga.edu/wp-content/uploads/2021/06/valero2021health.pdf

[12] S. Baker, W. Xiang, and I. Atkinson, "A hybrid neural network for continuous and non-invasive estimation of blood pressure from raw electrocardiogram and photoplethysmogram waveforms," *Computer Methods and Programs in Biomedicine*, vol. 207, p. 106191, 2021.

[13] A. M. Dart and B. A. Kingwell, "Pulse pressure—a review of mechanisms and clinical relevance," *Journal of the American College of Cardiology*, vol. 37, no. 4, pp. 975–984, 2001.

[14] J. Blacher, J. A. Staessen, X. Girerd, J. Gasowski, L. Thijs, L. Liu, J. G. Wang, R. H. Fagard, and M. E. Safar, "Pulse pressure not mean pressure determines cardiovascular risk in older hypertensive patients," *Archives of internal medicine*, vol. 160, no. 8, pp. 1085–1089, 2000.

[15] D. P. Kingma and J. Ba, "Adam: A method for stochastic optimization," *arXiv preprint arXiv:1412.6980*, 2014.

[16] S. Bai, J. Z. Kolter, and V. Koltun, "An empirical evaluation of generic convolutional and recurrent networks for sequence modeling," *arXiv preprint arXiv:1803.01271*, 2018.

[17] W. B. White, A. S. Berson, C. Robbins, M. J. Jamieson, L. M. Prisant, E. Roccella, and S. G. Sheps, "National standard for measurement of resting and ambulatory blood pressures with automated sphygmomanometers." *Hypertension*, vol. 21, no. 4, pp. 504–509, 1993.

[18] L. M. Prisant, B. S. Alpert, C. B. Robbins, A. S. Berson, M. Hayes, M. L. Cohen, and S. G. Sheps, "American national standard for nonautomated sphygmomanometers summary report," *American journal of hypertension*, vol. 8, no. 2, pp. 210–213, 1995.

[19] E. O'Brien, J. Petrie, W. Littler, M. de Swiet, P. L. Padfield, D. Altman, M. Bland, A. Coats, N. Atkins *et al.*, "The british hypertension society protocol for the evaluation of blood pressure measuring devices," *J hypertens*, vol. 11, no. Suppl 2, pp. S43–S62, 1993.

[20] J. Wang, Z. Wang, J. Li, and J. Wu, "Multilevel wavelet decomposition network for interpretable time series analysis," in *Proceedings of the 24th ACM SIGKDD International Conference on Knowledge Discovery & Data Mining*, 2018, pp. 2437–2446.

[21] X. Zou, Z. Wang, Q. Li, and W. Sheng, "Integration of residual network and convolutional neural network along with various activation functions and global pooling for time series classification," *Neurocomputing*, vol. 367, pp. 39–45, 2019.

[22] J. Surendiran, S. Theetchenya, P. Benson Mansingh, G. Sekar, M. Dhipa, N. Yuvaraj, V. Arulkarthick, C. Suresh, A. Sriram, K. Srihari *et al.*, "Segmentation of optic disc and cup using modified recurrent neural network," *BioMed Research International*, vol. 2022, 2022.

[23] K. Fauvel, T. Lin, V. Masson, É. Fromont, and A. Termier, "Xcm: An explainable convolutional neural network for multivariate time series classification," *Mathematics*, vol. 9, no. 23, p. 3137, 2021.

[24] G. Zerveas, S. Jayaraman, D. Patel, A. Bhamidipaty, and C. Eickhoff, "A transformer-based framework for multivariate time series representation learning," in *Proceedings of the 27th ACM SIGKDD Conference on Knowledge Discovery & Data Mining*, 2021, pp. 2114–2124.